

Supplementary Material

Dehydrochlorination of 1,2-dichloroethane over tetraphenylphosphonium chloride supported carbon catalyst

Yanzhao Dong ^a, Wei Zhao ^b, You Han ^a, Jinli Zhang ^{a, c}, Yao Nian ^a, Haiyang Zhang ^c, Wei Li ^{a*}

a. Key Laboratory for Green Chemical Technology MOE; School of Chemical Engineering & Technology, Tianjin University; Collaborative Innovation Center of Chemical Science and Chemical Engineering (Tianjin), Tianjin 300350, PR China.

b. Department of Research and Development, Zhuhai Coslight Battery Co., Ltd, Zhuhai 519100, PR China.

c. School of Chemistry and Chemical Engineering of Shihezi University, Shihezi, Xinjiang 832000, PR China.

* Corresponding author.

Fax: +86-22-2740-3389; Tel: +86-22-2740-4495;

E-mail address: liwei@tju.edu.cn (W. Li)

Table of contents:

Table S1 Initial catalytic activity of various quaternary phosphonium salts supported on AC.

Table. S2 The positions of relevant FT-IR peaks of pure TPPC and Fresh TPPC/AC samples.

Table S3 Desorption amount of the catalysts, determined by TPD measurement.

Fig. S1 Chemical structures of quaternary phosphonium salts used in our work.

Fig. S2 Effect of internal diffusion factor.

Fig. S3 Effect of external diffusion factor.

Fig. S4 (a) Effect of temperature on catalytic performance of 15%TPPC/AC catalyst;

(b) Effect of space velocity on catalytic performance of 15%TPPC/AC catalyst.

Fig. S5 Stability test of TPPC/AC for 360 h and its catalytic activity after regeneration treatment with diluted air.

Fig. S6 XPS spectra for fresh and used 15%TPPC/AC catalysts. (a) The total XPS spectra; (b) P 2p XPS spectra.

Fig. S7 Fourier transform infrared spectrometry (FT-IR) of TPPC, fresh 15%TPPC/AC and used 15%TPPC/AC catalysts.

Fig. S8 Nitrogen adsorption-desorption isotherms of 15%TPPC/AC and 5:10-N-AC catalysts.

Fig. S9 NH₃-TPD curves for N-AC and TPPC/AC catalysts.

Fig. S10 TGA profiles of the fresh and treated 15%TPPC/AC and 5:10-N-AC catalyst samples.

Fig. S11 The geometric structure of the substances involved in the pathway of the EDC pyrolysis process.

Table S1 Initial catalytic activity of various quaternary phosphonium salts supported on AC ^a.

Quaternary phosphonium salts/AC	Loading amount (wt%)	Conversion of EDC (%)	TOF (min ⁻¹)
AC	/	0.2	/
TPPC/AC	1.14	6.2	0.517
TMPC/AC	1.12	3.2	0.093
THPC/AC	1.12	0.6	0.026
MTPPB/AC	1.16	1.5	0.118
ETPPB/AC	1.18	1.4	0.112
PTPPB/AC	1.22	1.4	0.112
TPPB/AC	1.16	4.6	0.426
5:10-N-AC	4.90 ^b	15.8	0.023

a. Quaternary phosphonium salt catalysts, reaction conditions: $p=0.1$ MPa; $T=240$ °C; LHSV(EDC)= 0.6 h⁻¹. 5:10-N-AC catalyst ¹, reaction conditions: $p=0.1$ MPa; $T=240$ °C; LHSV(EDC)= 1.2 h⁻¹. The mass of catalyst is 5.0 g.

b. N element mass content determined by XPS.

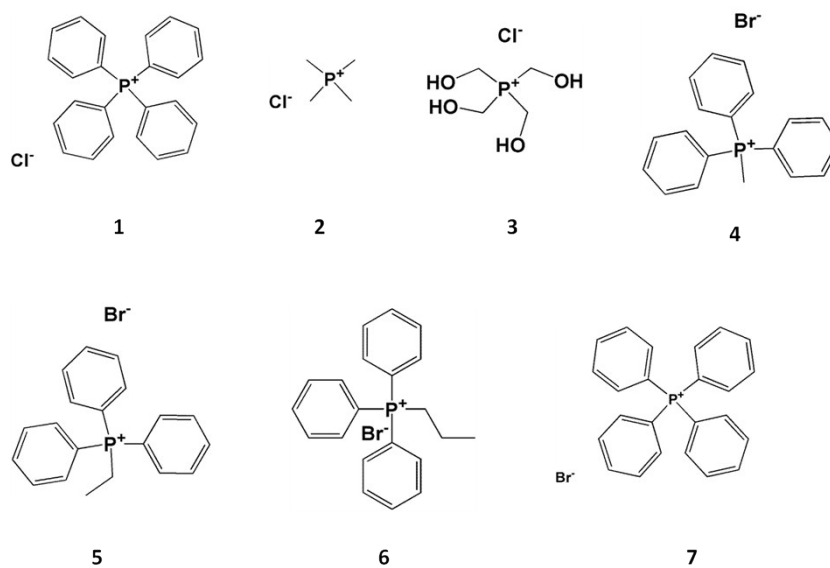


Fig. S1 Chemical structures of quaternary phosphonium salts used in our work. 1. TPPC; 2. TMPC; 3. THPC; 4. MTPPB; 5. ETPPB; 6. PTPPB; 7. TPPB.

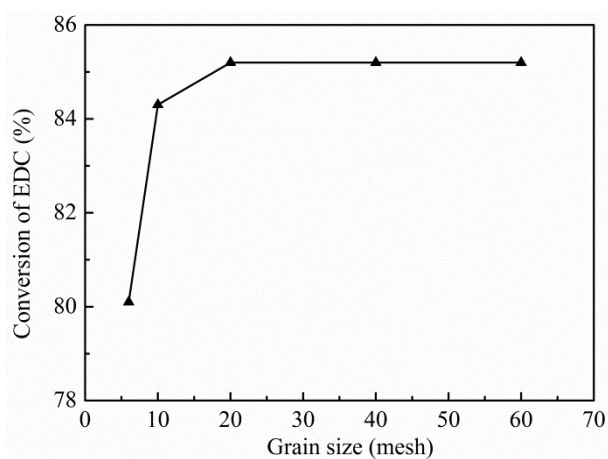


Fig. S2 Effect of internal diffusion factor. Reaction conditions: 240 °C, 0.1 MPa, the mass of each catalyst sample: 15 g; EDC volume flow rate: 0.1 mL min⁻¹.

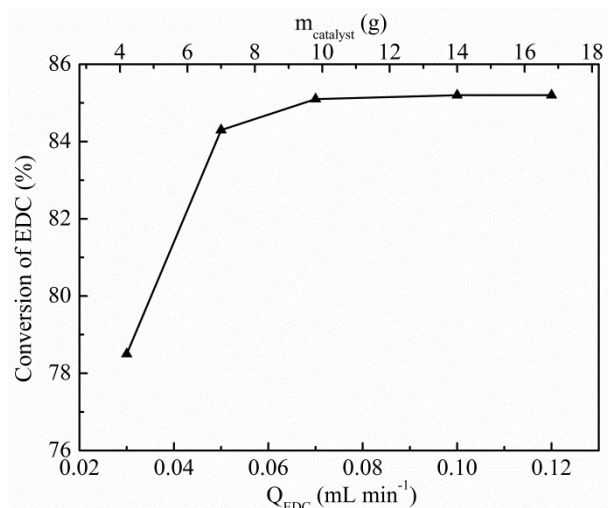


Fig. S3 Effect of external diffusion factor. Reaction conditions: 40-60 mesh, 240 °C, 0.1 MPa. (Q : volumetric flow rate of EDC; m : mass of catalyst).

Influence of temperature and space velocity on the catalytic activity

Fig. S4 (a) shows the catalytic activity of the prepared 15%TPPC/AC catalyst at different temperatures. As shown in Fig. S4(a), the EDC conversion swiftly increases from 6.8% to 99.9% as the reaction temperature increases from 180 °C to 250 °C. The selectivity to VCM decreases slightly from 99.6% to 99.1% as the reaction temperature increases from 180 °C to 280 °C.

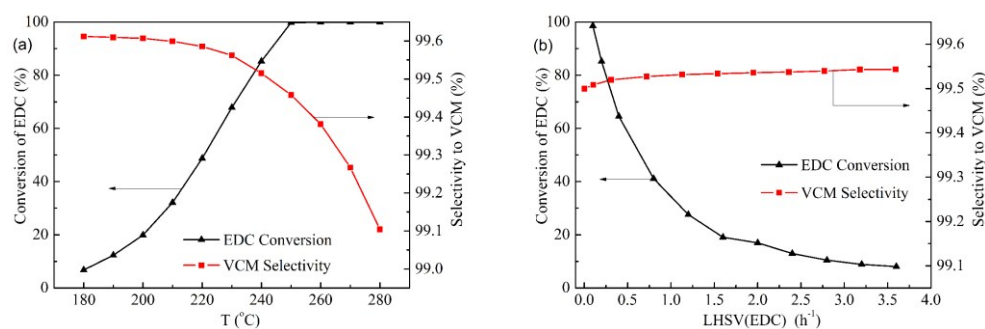


Fig. S4 (a) Effect of temperature on catalytic performance of 15%TPPC/AC catalyst; (b) Effect of space velocity on catalytic performance of 15%TPPC/AC catalyst.

Fig. S4 (b) shows the catalytic activity of the prepared 15%TPPC/AC catalyst at different EDC liquid hourly space velocity. As shown in Fig. S4(b), the EDC conversion dramatically decreases from 98.6% to 8.1% as the LHSV(EDC) increases from 0.1 h⁻¹ to 3.6 h⁻¹. But the selectivity to VCM increases slightly during the increase of LHSV(EDC).

The regeneration process was as follows:

The used catalyst was put into ceramic boat and was heated from 50 to 350 °C with a ramp rate of 3 °C min⁻¹ and then holding this final temperature for 2 h.

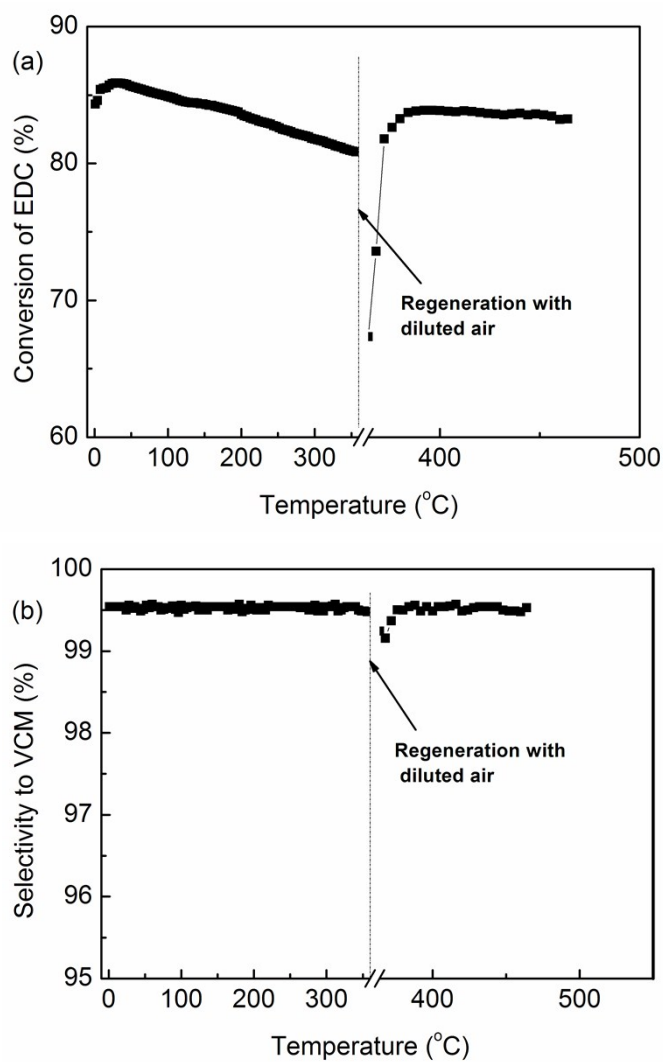


Fig. S5 Stability test of TPPC/AC for 360 h and its catalytic activity after regeneration treatment with diluted air. Reaction conditions: pressure (p)=0.1 MPa, temperature (T)=240 °C and LHSV(EDC)=0.2 h⁻¹.

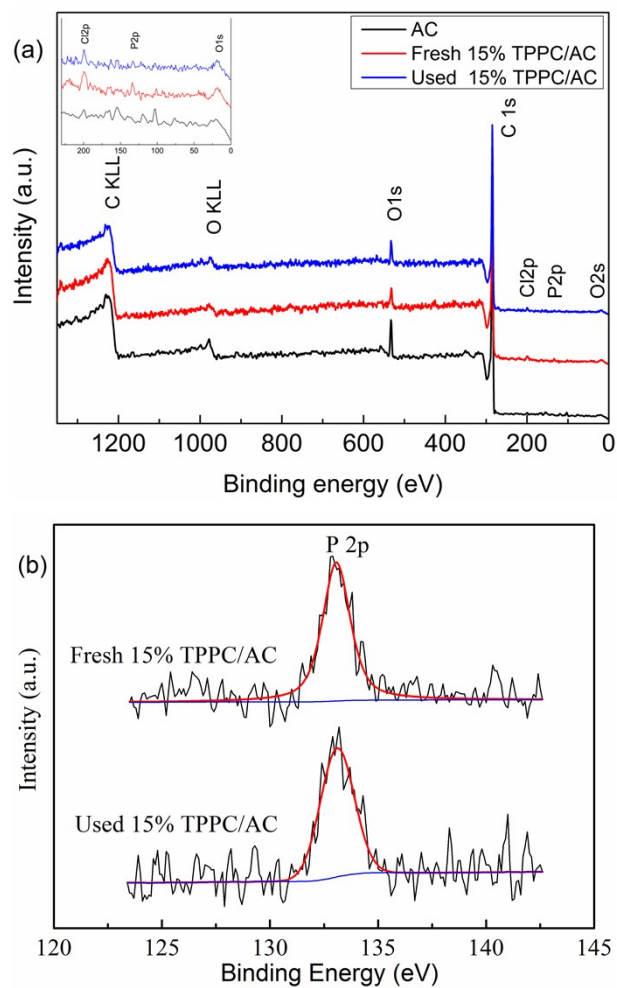


Fig. S6 XPS spectra for fresh and used 15%TPPC/AC samples. (a) The total XPS spectra; (b) P 2p XPS spectra.

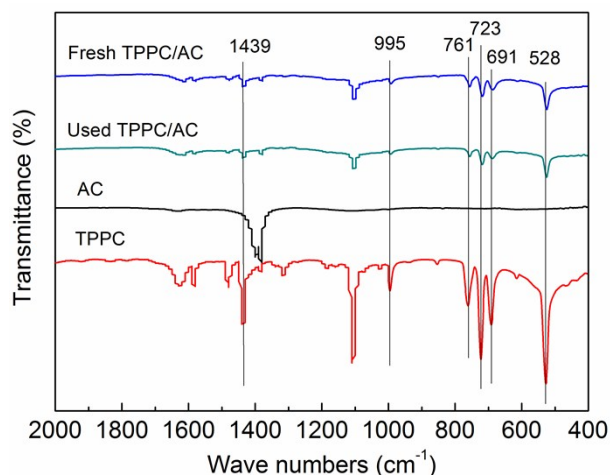


Fig. S7 Fourier transform infrared spectrometry (FT-IR) of TPPC, fresh 15%TPPC/AC and used 15%TPPC/AC catalysts.

As shown in Fig. S7, three peaks at 761 cm^{-1} , 723 cm^{-1} and 691 cm^{-1} are assigned to the bending vibration of benzene ring (C-H)². The peaks at 1439 cm^{-1} , 1582 cm^{-1} and 1430 cm^{-1} are ascribed to the stretching vibration of benzene skeleton (C-C) and the peak at 1107 cm^{-1} is due to the stretching vibration of C-P bond. It can be found that the main vibrational peaks of TPPC all appear on fresh and used TPPC/AC samples. This further confirms that TPPC has been supported on the AC support successfully. In addition, these vibrational peaks are all slightly red-shifted (Table S2). For example, the peaks at 528 cm^{-1} , 995 cm^{-1} and 1439 cm^{-1} are all shifted 2 cm^{-1} . The peaks at 723 cm^{-1} and 761 cm^{-1} are both shifted 5 cm^{-1} , and the peak at 691 cm^{-1} is shifted 4 cm^{-1} . These shifts indicate that there may be some interaction between TPPC and AC support³.

Table. S2 The positions of relevant FT-IR peaks of pure TPPC and Fresh TPPC/AC samples.

TPPC (cm^{-1})	Fresh TPPC/AC (cm^{-1})
528	526
691	687
723	718
761	756
995	993
1439	1437

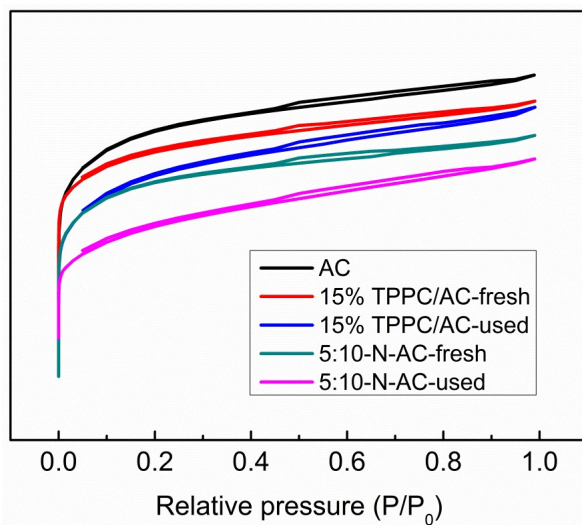


Fig. S8 Nitrogen adsorption-desorption isotherms of 15%TPPC/AC and 5:10-N-AC catalysts. All samples present type I isotherms, which is due to abundant micropore structure in activated carbon material.

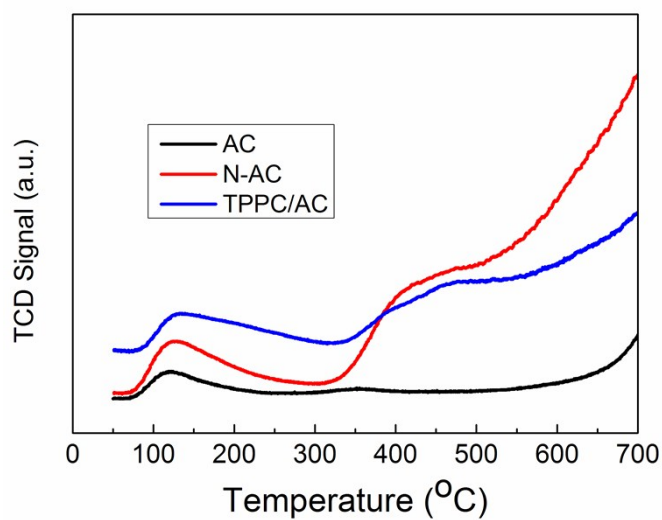


Fig. S9 NH₃-TPD curves for N-AC and TPPC/AC catalysts.

Estimation of coke accumulation after being treated in VCM and VCM-HCl gas mixture

To further confirm that the coke deposition could be ascribed to the diffusion problems in the removal of reaction products VCM and HCl, we performed the following exposed experiment based on the assumption of 100% conversion of EDC under the conditions of 0.1 MPa, 240 °C and an EDC liquid hourly space velocity of 0.2 h⁻¹.

Experiment process

After 30 mL (~15 g) catalyst sample was loaded into the micro-reactor unit, the reactor bed was heated and controlled at 240 °C in N₂ atmosphere. Then, VCM (27.9 mL min⁻¹) or VCM-HCl mixture gases (VCN: 27.9 mL min⁻¹, HCl: 27.9 mL min⁻¹) was delivered into the reactor. The treatment process was maintained for 60 h at 240 °C. After the pretreatment operation, the thermogravimetric analysis was carried out to measure the amount of coke deposition. The detailed analysis and calculation process are the same as our previous method⁴⁻⁶.

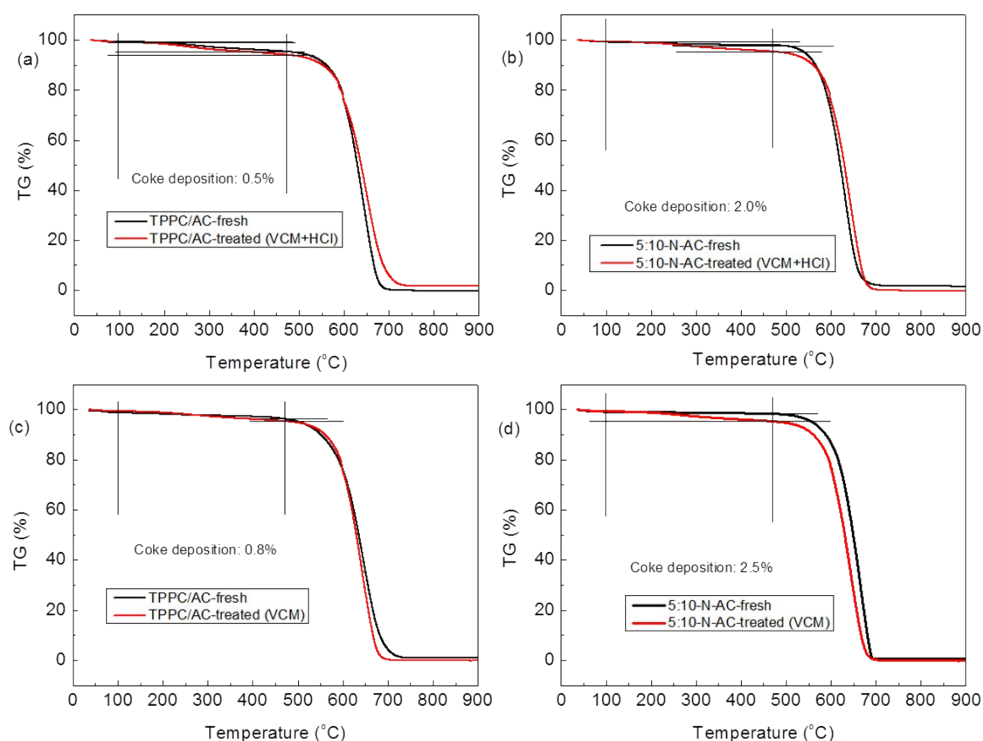


Fig. S10 TGA profiles of the fresh and treated 15%TPPC/AC and 5:10-N-AC catalyst samples. The catalyst samples were treated in VCM-HCl mixture gases (a) and (b); The catalyst sample were treated in VCM gas (c) and (d).

Table S3 Desorption amount of the catalysts, determined by TPD measurement.

Samples	Desorption area of VCM	Desorption area of HCl
15%TPPC/AC	3166	4286
5:10-N-AC	5423	1836

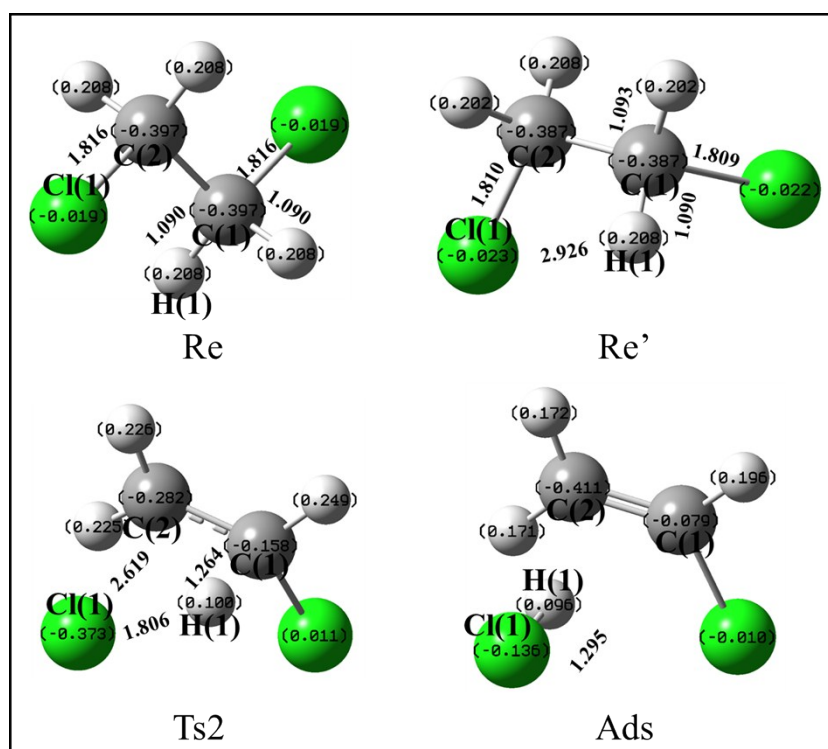


Fig. S11 The geometric structure of the substances involved in the pathway of the EDC pyrolysis process. The initial structure of EDC (Re), the second configuration of EDC (Re'), transition state (Ts2), the adsorbed structure of HCl and VCM products (Ads). Green, gray and white globule represents chlorine, carbon and hydrogen atom, respectively.

References

1. W. Zhao, M. Sun, H. Zhang, Y. Dong, X. Li, W. Li and J. Zhang, *RSC Adv.*, 2015, **5**, 104071-104078.
2. X. Cai, S. Tan, M. Lin, A. Xie, W. Mai, X. Zhang, Z. Lin, T. Wu and Y. Liu, *Langmuir*, 2011, **27**, 7828-7835.
3. M. Mauro, M. Maggio, A. Antonelli, M. R. Acocella and G. Guerra, *Chem. Mater.*, 2015, **27**, 1590-1596.
4. Y. Dong, W. Li, Z. Yan and J. Zhang, *Catal. Sci. Technol.*, 2016, **6**, 7946-7955.
5. Y. Z. Dong, H. Y. Zhang, W. Li, M. X. Sun, C. L. Guo and J. L. Zhang, *J. Ind. Eng. Chem.*, 2016, **35**, 177-184.
6. G. Li, W. Li and J. Zhang, *Catal. Sci. Technol.*, 2016, **6**, 1821-1828.